University of Kentucky
UKnowledge

Physics and Astronomy Faculty Publications   Physics and Astronomy

2-24-2016

Probing Parton Dynamics of QCD Matter with Ω and φ Production

L. Adamczyk
AGH University of Science and Technology, Poland

James K. Adkins
University of Kentucky, kevin.adkins@uky.edu

G. Agakishiev
Joint Institute for Nuclear Research, Russia

M. M. Aggarwal
Panjab University, India

Z. Ahammed
Variable Energy Cyclotron Centre, India

See next page for additional authors

Click here to let us know how access to this document benefits you.

Follow this and additional works at: https://uknowledge.uky.edu/physastron_facpub

Part of the Nuclear Commons

Authors

L. Adamczyk, James K. Adkins, G. Agakishiev, M. M. Aggarwal, Z. Ahammed, I. Alekseev, A. Aparin, D. Arkhipkin, E. C. Aschenauer, A. Attri, G. S. Averichev, X. Bai, V. Bairathi, R. Bellwied, A. Bhasin, A. K. Bhati, P. Bhattarai, J. Bielcik, J. Bielcikova, L. C. Bland, I. G. Bordyuzhin, J. Bouchet, J. D. Brandenburg, A. V. Brandin, I. Bunzarov, J. Butterworth, H. Caines, M. Calderón de la Barca Sánchez, J. M. Campbell, D. Cebra, Renee H. Fatemi, and Suvarna Ramachandran

Probing Parton Dynamics of QCD Matter with Ω and ϕ Production

Due to the large number of authors, only the first 30 and the authors affiliated with the University of Kentucky are listed in the author section above. For the complete list of authors, please download this article.

The authors of this article are collectively known as STAR Collaboration.

Probing parton dynamics of QCD matter with Ω and φ production

L. Adamczyk,[1] J. K. Adkins,[20] G. Agakishiev,[18] M. M. Aggarwal,[31] Z. Ahammed,[49] I. Alekseev,[16] A. Aparin,[18] D. Arkhipkin,[3] E. C. Aschenauer,[3] A. Attri,[31] G. S. Averichev,[18] X. Bai,[7] V. Bairathi,[27] R. Bellwied,[45] A. Bhasin,[17] A. K. Bhati,[31] P. Bhattarai,[44] J. Bielcik,[10] J. Bielcikova,[11] L. C. Bland,[3] I. G. Bordyuzhin,[16] J. Bouchet,[19] J. D. Brandenburg,[37] A. V. Brandin,[26] I. Bunzarov,[18] J. Butterworth,[37] H. Caines,[53] M. Calderón de la Barca Sánchez,[5] J. M. Campbell,[29] D. Cebra,[5] I. Chakaberia,[3] P. Chaloupka,[10] Z. Chang,[43] A. Chatterjee,[49] S. Chattopadhyay,[49] J. H. Chen,[40] X. Chen,[22] J. Cheng,[46] M. Cherney,[9] W. Christie,[3] G. Contin,[23] H. J. Crawford,[4] S. Das,[13] L. C. De Silva,[9] R. R. Debbe,[3] T. G. Dedovich,[18] J. Deng,[39] A. A. Derevschikov,[33] B. di Ruzza,[3] L. Didenko,[3] C. Dilks,[32] X. Dong,[23] J. L. Drachenberg,[48] J. E. Draper,[5] C. M. Du,[22] L. E. Dunkelberger,[6] J. C. Dunlop,[3] L. G. Efimov,[18] J. Engelage,[4] G. Eppley,[37] R. Esha,[6] O. Evdokimov,[8] O. Eyser,[3] R. Fatemi,[20] S. Fazio,[3] P. Federic,[11] J. Fedorisin,[18] Z. Feng,[7] P. Filip,[18] Y. Fisyak,[3] C. E. Flores,[5] L. Fulek,[1] C. A. Gagliardi,[43] D. Garand,[34] F. Geurts,[37] A. Gibson,[48] M. Girard,[50] L. Greiner,[23] D. Grosnick,[48] D. S. Gunarathne,[42] Y. Guo,[38] S. Gupta,[17] A. Gupta,[17] W. Guryn,[3] A. I. Hamad,[19] A. Hamed,[43] R. Haque,[27] J. W. Harris,[53] L. He,[34] S. Heppelmann,[5] S. Heppelmann,[32] A. Hirsch,[34] G. W. Hoffmann,[44] S. Horvat,[53] T. Huang,[28] X. Huang,[46] B. Huang,[8] H. Z. Huang,[6] P. Huck,[7] T. J. Humanic,[29] G. Igo,[6] W. W. Jacobs,[15] H. Jang,[21] A. Jentsch,[44] J. Jia,[3] K. Jiang,[38] E. G. Judd,[4] S. Kabana,[19] D. Kalinkin,[15] K. Kang,[46] K. Kauder,[51] H. W. Ke,[3] D. Keane,[19] A. Kechechyan,[18] Z. H. Khan,[8] D. P. Kiková,[50] I. Kisel,[12] A. Kisiel,[50] L. Kochenda,[26] D. D. Koetke,[48] L. K. Kosarzewski,[50] A. F. Kraishan,[42] P. Kravtsov,[26] K. Krueger,[2] L. Kumar,[31] M. A. C. Lamont,[3] J. M. Landgraf,[3] K. D. Landry,[6] J. Lauret,[3] A. Lebedev,[3] R. Lednicky,[18] J. H. Lee,[3] X. Li,[42] C. Li,[38] X. Li,[38] Y. Li,[46] W. Li,[40] T. Lin,[15] M. A. Lisa,[29] F. Liu,[7] T. Ljubicic,[3] W. J. Llope,[51] M. Lomnitz,[19] R. S. Longacre,[3] X. Luo,[7] R. Ma,[3] G. L. Ma,[40] Y. G. Ma,[40] L. Ma,[40] N. Magdy,[41] R. Majka,[53] A. Manion,[23] S. Margetis,[19] C. Markert,[44] H. S. Matis,[23] D. McDonald,[45] S. McKinzie,[23] K. Meehan,[5] J. C. Mei,[39] N. G. Minaev,[33] S. Mioduszewski,[43] D. Mishra,[27] B. Mohanty,[27] M. M. Mondal,[43] D. A. Morozov,[33] M. K. Mustafa,[23] B. K. Nandi,[14] Md. Nasim,[6] T. K. Nayak,[49] G. Nigmatkulov,[26] T. Niida,[51] L. V. Nogach,[33] S. Y. Noh,[21] J. Novak,[25] S. B. Nurushev,[33] G. Odyniec,[23] A. Ogawa,[3] K. Oh,[35] V. A. Okorokov,[26] D. Olvitt Jr.,[42] B. S. Page,[3] R. Pak,[3] Y. X. Pan,[6] Y. Pandit,[8] Y. Panebratsev,[18] B. Pawlik,[30] H. Pei,[7] C. Perkins,[4] P. Pile,[3] J. Pluta,[50] K. Poniatowska,[50] J. Porter,[23] M. Posik,[42] A. M. Poskanzer,[23] N. K. Pruthi,[31] J. Putschke,[51] H. Qiu,[23] A. Quintero,[19] S. Ramachandran,[20] S. Raniwala,[36] R. Raniwala,[36] R. L. Ray,[44] H. G. Ritter,[23] J. B. Roberts,[37] O. V. Rogachevskiy,[18] J. L. Romero,[5] L. Ruan,[3] J. Rusnak,[11] O. Rusnakova,[10] N. R. Sahoo,[43] P. K. Sahu,[13] I. Sakrejda,[23] S. Salur,[23] J. Sandweiss,[53] A. Sarkar,[14] J. Schambach,[44] R. P. Scharenberg,[34] A. M. Schmah,[23] W. B. Schmidke,[3] N. Schmitz,[24] J. Seger,[9] P. Seyboth,[24] N. Shah,[40] E. Shahaliev,[18] P. V. Shanmuganathan,[19] M. Shao,[38] A. Sharma,[17] B. Sharma,[31] M. K. Sharma,[17] W. Q. Shen,[40] Z. Shi,[23] S. S. Shi,[7] Q. Y. Shou,[40] E. P. Sichtermann,[23] R. Sikora,[1] M. Simko,[11] S. Singha,[19] M. J. Skoby,[15] N. Smirnov,[53] D. Smirnov,[3] W. Solyst,[15] L. Song,[45] P. Sorensen,[3] H. M. Spinka,[2] B. Srivastava,[34] T. D. S. Stanislaus,[48] M. Stepanov,[34] R. Stock,[12] M. Strikhanov,[26] B. Stringfellow,[34] M. Sumbera,[11] B. Summa,[32] Z. Sun,[22] X. M. Sun,[7] Y. Sun,[38] B. Surrow,[42] D. N. Svirida,[16] Z. Tang,[38] A. H. Tang,[3] T. Tarnowsky,[25] A. Tawfik,[52] J. Thäder,[23] J. H. Thomas,[23] A. R. Timmins,[45] T. Todoroki,[3] M. Tokarev,[18] S. Trentalange,[6] R. E. Tribble,[43] P. Tribedy,[3] S. K. Tripathy,[13] O. D. Tsai,[6] T. Ullrich,[3] D. G. Underwood,[2] I. Upsal,[29] G. Van Buren,[3] G. van Nieuwenhuizen,[3] M. Vandenbroucke,[42] R. Varma,[14] A. N. Vasiliev,[33] R. Vertesi,[11] F. Videbæk,[3] S. Vokal,[18] S. A. Voloshin,[51] A. Vossen,[15] F. Wang,[34] G. Wang,[6] J. S. Wang,[22] H. Wang,[3] Y. Wang,[7] Y. Wang,[46] G. Webb,[3] J. C. Webb,[3] L. Wen,[6] G. D. Westfall,[25] H. Wieman,[23] S. W. Wissink,[15] R. Witt,[47] Y. Wu,[19] Z. G. Xiao,[46] W. Xie,[34] G. Xie,[38] K. Xin,[37] Y. F. Xu,[40] Q. H. Xu,[39] N. Xu,[23] H. Xu,[22] Z. Xu,[3] J. Xu,[7] S. Yang,[38] Y. Yang,[28] Y. Yang,[7] C. Yang,[38] Y. Yang,[22] Q. Yang,[38] Z. Ye,[8] Z. Ye,[8] P. Yepes,[37] L. Yi,[53] K. Yip,[3] I.-K. Yoo,[35] N. Yu,[7] H. Zbroszczyk,[50] W. Zha,[38] X. P. Zhang,[46] Y. Zhang,[38] J. Zhang,[39] J. Zhang,[22] S. Zhang,[40] S. Zhang,[38] Z. Zhang,[40] J. B. Zhang,[7] F. Zhao,[6] J. Zhao,[34] C. Zhong,[40] L. Zhou,[38] X. Zhu,[46] Y. Zoulkarneeva,[18] and M. Zyzak[12]

(STAR Collaboration)

[1]*AGH University of Science and Technology, FPACS, Cracow 30-059, Poland*
[2]*Argonne National Laboratory, Argonne, Illinois 60439, USA*
[3]*Brookhaven National Laboratory, Upton, New York 11973, USA*
[4]*University of California, Berkeley, California 94720, USA*
[5]*University of California, Davis, California 95616, USA*
[6]*University of California, Los Angeles, California 90095, USA*
[7]*Central China Normal University, Wuhan, Hubei 430079, China*
[8]*University of Illinois at Chicago, Chicago, Illinois 60607, USA*
[9]*Creighton University, Omaha, Nebraska 68178, USA*
[10]*Czech Technical University in Prague, FNSPE, Prague, 115 19, Czech Republic*
[11]*Nuclear Physics Institute AS CR, 250 68 Prague, Czech Republic*
[12]*Frankfurt Institute for Advanced Studies FIAS, Frankfurt 60438, Germany*
[13]*Institute of Physics, Bhubaneswar 751005, India*
[14]*Indian Institute of Technology, Mumbai 400076, India*
[15]*Indiana University, Bloomington, Indiana 47408, USA*
[16]*Alikhanov Institute for Theoretical and Experimental Physics, Moscow 117218, Russia*

[17] *University of Jammu, Jammu 180001, India*

[18] *Joint Institute for Nuclear Research, Dubna, 141 980, Russia*

[19] *Kent State University, Kent, Ohio 44242, USA*

[20] *University of Kentucky, Lexington, Kentucky, 40506-0055, USA*

[21] *Korea Institute of Science and Technology Information, Daejeon 305-701, Korea*

[22] *Institute of Modern Physics, Chinese Academy of Sciences, Lanzhou, Gansu 730000, China*

[23] *Lawrence Berkeley National Laboratory, Berkeley, California 94720, USA*

[24] *Max-Planck-Institut fur Physik, Munich 80805, Germany*

[25] *Michigan State University, East Lansing, Michigan 48824, USA*

[26] *National Research Nuclear Univeristy MEPhI, Moscow 115409, Russia*

[27] *National Institute of Science Education and Research, Bhubaneswar 751005, India*

[28] *National Cheng Kung University, Tainan 70101, Taiwan*

[29] *Ohio State University, Columbus, Ohio 43210, USA*

[30] *Institute of Nuclear Physics PAN, Cracow 31-342, Poland*

[31] *Panjab University, Chandigarh 160014, India*

[32] *Pennsylvania State University, University Park, Pennsylvania 16802, USA*

[33] *Institute of High Energy Physics, Protvino 142281, Russia*

[34] *Purdue University, West Lafayette, Indiana 47907, USA*

[35] *Pusan National University, Pusan 46241, Korea*

[36] *University of Rajasthan, Jaipur 302004, India*

[37] *Rice University, Houston, Texas 77251, USA*

[38] *University of Science and Technology of China, Hefei, Anhui 230026, China*

[39] *Shandong University, Jinan, Shandong 250100, China*

[40] *Shanghai Institute of Applied Physics, Chinese Academy of Sciences, Shanghai 201800, China*

[41] *State University Of New York, Stony Brook, New York 11794, USA*

[42] *Temple University, Philadelphia, Pennsylvania 19122, USA*

[43] *Texas A&M University, College Station, Texas 77843, USA*

[44] *University of Texas, Austin, Texas 78712, USA*

[45] *University of Houston, Houston, Texas 77204, USA*

[46] *Tsinghua University, Beijing 100084, China*

[47] *United States Naval Academy, Annapolis, Maryland, 21402, USA*

[48] *Valparaiso University, Valparaiso, Indiana 46383, USA*

[49] *Variable Energy Cyclotron Centre, Kolkata 700064, India*

[50] *Warsaw University of Technology, Warsaw 00-661, Poland*

[51] *Wayne State University, Detroit, Michigan 48201, USA*

[52] *World Laboratory for Cosmology and Particle Physics (WLCAPP), Cairo 11571, Egypt*

[53] *Yale University, New Haven, Connecticut 06520, USA*

We present measurements of Ω and ϕ production at midrapidity from Au+Au collisions at nucleon-nucleon center-of-mass energies $\sqrt{s_{NN}} = 7.7, 11.5, 19.6, 27,$ and 39 GeV by the STAR experiment at the BNL Relativistic Heavy Ion Collider (RHIC). Motivated by the coalescence formation mechanism for these strange hadrons, we study the ratios of $N(\Omega^- + \overline{\Omega}^+)/[2N(\phi)]$. These ratios as a function of transverse momentum p_T fall on a consistent trend at high collision energies, but start to show deviations in peripheral collisions at $\sqrt{s_{NN}} = 19.6,$ 27, and 39 GeV, and in central collisions at 11.5 GeV in the intermediate p_T region of $2.4-3.6$ GeV/c. We further evaluate empirically the strange quark p_T distributions at hadronization by studying the Ω/ϕ ratios scaled by the number of constituent quarks (NCQ). The NCQ-scaled Ω/ϕ ratios show a suppression of strange quark production in central collisions at 11.5 GeV compared to $\sqrt{s_{NN}} \geqslant 19.6$ GeV. The shapes of the presumably thermal strange quark distributions in 0–60% most central collisions at 7.7 GeV show significant deviations from those in 0–10% most central collisions at higher energies. These features suggest that there is likely a change of the underlying strange quark dynamics in the transition from quark matter to hadronic matter at collision energies below 19.6 GeV.

Lattice quantum chromodynamics (QCD) calculations suggest that at high temperature and low baryon chemical potential (μ_{B}), the transition from the quark gluon plasma (QGP) to the state of a hadron gas is smooth and continuous (cross-over transition) [1]. At lower temperatures and high μ_{B}, theoretical calculations predict a first order phase transition [2] which

may end at a critical point [3]. The mapping of the QCD phase diagram has been a subject of intensive theoretical and experimental activities in the past decades. In central Pb-Pb collisions at the CERN Super Proton Synchrotron (SPS), the enhanced production of Ω at $\sqrt{s_{NN}} = 8.8$ and 17.3 GeV [4–6] and ϕ mesons at $\sqrt{s_{NN}} = 6.3-17.3$ GeV [7] compared to π mesons has been considered as a QGP signal [8]. Multistrange hadrons such as $\Omega(sss)$ hyperons and $\phi(s\bar{s})$ mesons are important probes for the search of the QCD phase boundaries [9,10]. The Ω hyperons and ϕ mesons are expected to have relatively small hadronic interaction cross sections [11,12]. Therefore, they can carry the information directly from the chemical freeze-out stage with little or no distortion due to hadronic rescattering. In addition, the measured Ω and ϕ yields suffer minimal distortion from decay feed-down. As a result, the production of the Ω and ϕ particles offers a unique advantage in probing the transition from partonic to hadronic dynamics.

In heavy ion collisions at the top RHIC energy of $\sqrt{s_{NN}} = 200$ GeV, model calculations [13–17] and experimental data suggest that particles at intermediate p_T are formed via the coalescence of low p_T quarks from the bulk partonic matter and/or fragmented hard partons. Experimentally, baryon to meson ratios have been found to be large compared to those from elementary collisions [9,18–21]. The measured elliptic flow v_2 has been found to scale with the number of constituent quarks (NCQ) for both baryons and mesons [22] in Au+Au collisions at the top RHIC energy. In order to explain these observations, coalescence model calculations require the development of collectivity among constituent quarks during the partonic phase. This partonic collectivity has been considered as an important evidence for the formation of deconfined QCD matter with partonic degrees of freedom in Au+Au collisions at the highest RHIC energy [9,18–21].

In order to map out the phase diagram of the QCD matter, a Beam Energy Scan (BES) program has been initiated at RHIC with Au+Au collisions at $\sqrt{s_{NN}} = 7.7-39$ GeV [23]. These collisions allow us to reach a broad range of temperature and μ_B in the QCD phase diagram [24] and search for a possible beam energy region where the underlying dynamics are different from those of partonic matter observed in Au+Au collisions at the top RHIC energy.

The STAR experiment [25] collected Au+Au collision data at $\sqrt{s_{NN}} = 7.7$, 11.5, and 39 GeV in 2010, and 19.6 and 27 GeV in 2011. As a collider detector, STAR has uniform acceptance over different beam energies and extensive reach to intermediate p_T range for both Ω and ϕ particles. In this Rapid Communication we present the first RHIC measurements of midrapidity ($|y| < 0.5$) Ω and ϕ production for various collision centrality intervals from the BES.

A minimum bias trigger for the collision data sample was defined using a coincidence of signals from either the zero degree calorimeters, vertex position detectors, or beam-beam counters [26,27]. STAR's time projection chamber (TPC) [25] was used for tracking of charged particles and particle identification. In the offline data analysis, we required the radial position of the reconstructed primary vertex to be within 2 cm of the beam axis to suppress events from collisions with the beam pipe (radius of 3.95 cm). To ensure nearly uniform detector acceptance, the analyzed events were required to have
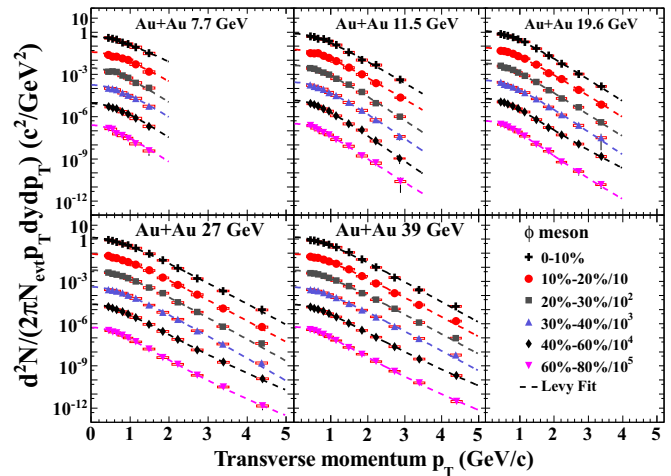

FIG. 1. Midrapidity ($|y| < 0.5$) ϕ meson p_T spectra from Au+Au collisions at different centralities and energies ($\sqrt{s_{NN}} = 7.7-39$ GeV). The red boxes represent systematic errors. The dashed curves represent fits to the experimental data with a Levy function [9].

a primary Z vertex (along the beam direction) within ± 70 cm from the center of the TPC for $\sqrt{s_{NN}} = 7.7$, 19.6, and 27 GeV collisions and ± 50 and ± 40 cm for $\sqrt{s_{NN}} = 11.5$ and 39 GeV, respectively. After the event selection, we obtained approximately $(4, 12, 36, 70, 130) \times 10^6$ Au+Au minimum bias triggered events at $\sqrt{s_{NN}} = 7.7$, 11.5, 19.6, 27, and 39 GeV, respectively. The collision centrality was determined by comparing the uncorrected charged hadron multiplicity measured from the TPC at midrapidity ($|\eta| < 0.5$) with Monte Carlo Glauber simulations [26,27].

The multistrange hadron signals and raw yields were obtained from the invariant mass distributions reconstructed through their hadronic decay channels: $\phi \to K^+ + K^-$ and $\Omega^-(\overline{\Omega}^+) \to \Lambda(\bar{\Lambda}) + K^-(K^+)$. The decay daughters $\Lambda(\bar{\Lambda})$ were reconstructed through $\Lambda(\bar{\Lambda}) \to p(\bar{p}) + \pi^-(\pi^+)$. Charged hadrons ($\pi^\pm, K^\pm, p, \bar{p}$) were identified by their specific energy loss (dE/dx) in the TPC gas [25]. The combinatorial background of the weakly decaying particles $\Lambda(\bar{\Lambda})$ and $\Omega^-(\overline{\Omega}^+)$ was reduced by geometrical cuts on their decay topology [27,28]. The $\Omega^-(\overline{\Omega}^+)$ combinatorial background was estimated by rotating $K^-(K^+)$ tracks at five different angles from $\pi/3$ to $5\pi/3$ and normalizing the invariant mass distribution to the mass window of (1.625, 1.655 GeV/c^2) and (1.69, 1.72 GeV/c^2). The $\Omega^-(\overline{\Omega}^+)$ raw yields were extracted by counting the signals within a mass window from 1.660 to 1.685 GeV/c^2 after subtracting the rotational background. The K^+K^- combinatorial background in ϕ meson reconstruction was subtracted with the mixed event technique [9,29]. The ϕ meson raw yields were determined by a Breit-Wigner + polynomial function (up to second order) fit to the mixed-event-background-subtracted K^+K^- invariant mass distribution [9,29].

Figures 1 and 2 show the p_T spectra of ϕ and $\Omega^-(\overline{\Omega}^+)$ at midrapidity ($|y| < 0.5$) for different centralities from Au+Au collisions at $\sqrt{s_{NN}} = 7.7-39$ GeV. The spectra were corrected
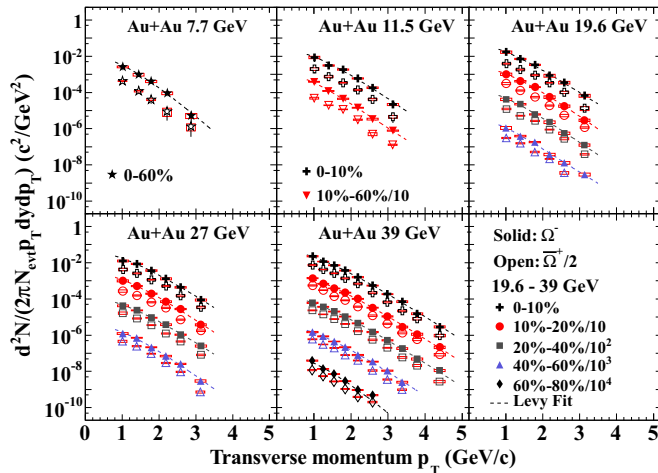
FIG. 2. Midrapidity ($|y| < 0.5$) Ω^- ($\overline{\Omega}^+$) p_T spectra from Au+Au collisions at different centralities and energies ($\sqrt{s_{NN}} = 7.7$–39 GeV). The open symbols represent $\overline{\Omega}^+$ and solid symbols represent Ω^-. The red boxes denote systematic errors. The dashed curves represent fits to the experimental data with a Levy function [9].

FIG. 3. Baryon-to-meson ratio, $N(\Omega^- + \overline{\Omega}^+)/[2N(\phi)]$, as a function of p_T in midrapidity ($|y| < 0.5$) from Au+Au collisions at $\sqrt{s_{NN}} = 7.7$–200 GeV. Error bars and boxes represent statistical and systematic uncertainties, respectively. Ω and ϕ systematic errors are mostly from uncorrelated contributions. The solid and dashed lines represent recombination model calculations for central collisions at $\sqrt{s_{NN}} = 200$ GeV [14] with total and thermal strange quark contributions, respectively.

for reconstruction efficiency and geometrical acceptance. The systematic errors mainly come from two sources: the different signal extraction techniques, and the reconstruction efficiency corrections. They were studied as a function of p_T and were obtained by exploring the dependence of invariant yields on various raw yield extraction techniques including different fit and counting ranges and different fit functions, and on different combinations of analysis cuts. For the ϕ meson, relative systematic errors of invariant yields vary from 10%–16% at $\sqrt{s_{NN}} = 11.5$–39 GeV to 17%–21% at $\sqrt{s_{NN}} = 7.7$ GeV. The systematic errors in 0–10% central collisions are generally larger than those in 60%–80% peripheral collisions by 2%–3% due to greater combinatorial backgrounds. For $p_T < 0.8$ GeV/c in central collisions, the uncertainty of ϕ meson raw yield extraction is dominant. However, for $p_T > 1.6$ GeV/c the main source of systematic error is the differences in track selection cuts. For the Ω invariant yields, the relative systematic errors vary from $\sim 5\%$ to 20%, and are dominated by the signal extraction methods. Due to the higher combinatorial background in $p_T \lesssim 1.2$ GeV/c and low statistics at $p_T \gtrsim 2.8$ GeV/c, the systematic errors are found to be larger in the corresponding p_T windows. The systematic uncertainties have a weak centrality dependence and their energy dependences for Ω and ϕ particles are similar. The systematic errors of invariant yields of ϕ and Ω are shown as red boxes in Figs. 1 and 2 for each p_T bin.

We present baryon-to-meson ratios of invariant yields, $N(\Omega^- + \overline{\Omega}^+)/[2N(\phi)]$, as a function of p_T from Au+Au collisions for various beam energies from $\sqrt{s_{NN}} = 7.7$ to 200 GeV in Fig. 3 and for various collision centralities in Fig. 4, respectively. Data from 200 GeV Au+Au collisions are from previously published STAR results [9]. Coalescence or recombination models [14,15, 26] have been used to describe particle productions in nucleus-nucleus collisions at RHIC. In particular, a model calculation by Hwa and Yang for Au+Au
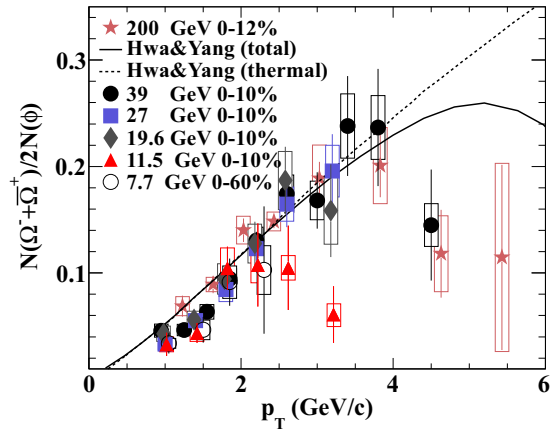
collisions at $\sqrt{s_{NN}} = 200$ GeV [14] predicts that Ω hyperons up to p_T of 6 GeV/c are dominated by the recombination of three thermal quarks while for ϕ mesons the thermal-shower quark recombination contributes significantly to p_T above 4 GeV/c which reduces the ratios at high p_T leading to the deviations from the straight line. Deviations from the theory calculation at low p_T could indicate that thermal strange quarks may not have an exponential distribution.

In Fig. 3 the measured $N(\Omega^- + \overline{\Omega}^+)/[2N(\phi)]$ ratios from central Au+Au collisions at $\sqrt{s_{NN}} = 19.6$, 27, and 39 GeV follow closely the ratio from 200 GeV and are consistent with a picture of coalescence and recombination dynamics over a broad p_T range of 1–4 GeV/c. The ratios at 11.5 GeV seem to deviate from the trend observed at higher beam energies. In particular, the ratios at 11.5 GeV appear to turn down around p_T of 2 GeV/c while those at higher beam energies such as 39 and 200 GeV peak at p_T of 3 GeV/c or above. The collision centrality dependence of the $N(\Omega^- + \overline{\Omega}^+)/[2N(\phi)]$ ratios in Figs. 4(a)–4(d) shows significant differences between the 40%–60% centrality bin and the other centrality intervals for Au+Au collisions at 19.6 and 27 GeV. Furthermore, the ratios from the peripheral collisions of 40%–60% at 27 GeV are similar in magnitude to the ratios from collisions at 11.5 GeV. Because the Ω and ϕ particles have small hadronic rescattering cross sections [30], the change in these ratios is likely to originate from the partonic phase. The decrease in the $N(\Omega^- + \overline{\Omega}^+)/[2N(\phi)]$ ratios from central collisions at 11.5 GeV compared to those at 19.6 GeV or above may indicate a significant change in the hadron formation dynamics and/or in strange quark p_T distributions at the lower energy. Such a change may arise from a transition from hadronic to partonic dynamics with increasing beam energy. The turnover in the ratios from Au+Au collisions below 11.5 GeV beam energy is unlikely to be due to contributions of high p_T shower partons
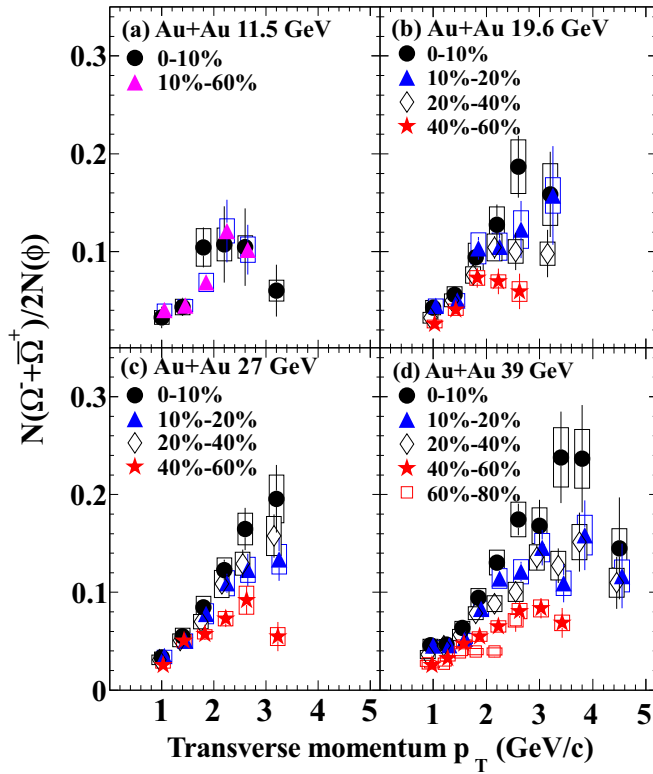
FIG. 4. Centrality dependence of $N(\Omega^- + \overline{\Omega}^+)/[2N(\phi)]$ ratios, as a function of p_T in midrapidity ($|y| < 0.5$) from Au+Au collisions at $\sqrt{s_{NN}} = 11.5, 19.6, 27$, and 39 GeV. The boxes denote systematic errors.
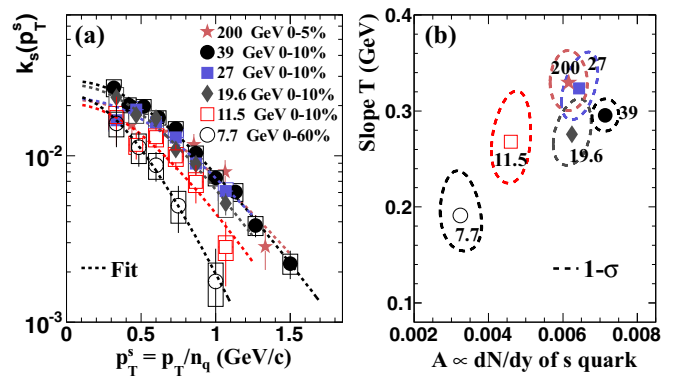

FIG. 5. (a) NCQ-scaled $N(\Omega^- + \overline{\Omega}^+)/[2N(\phi)]$ ratios, $k_s(p_T^s)$, as a function of p_T/n_q in midrapidity ($|y| < 0.5$) from Au+Au collisions at $\sqrt{s_{NN}} = 7.7$–200 GeV. Here n_q is the number of constituent quarks of each hadron. The boxes denote systematic errors. Dashed lines are Boltzmann fits to data. (b) The fitting parameters A and T, and 1σ contours (including statistic and systematic errors).

as suggested by model calculations from Hwa and Yang [14] because of relatively low p_T particles involved.

We illustrate qualitatively the change in the underlying bulk strange quark p_T distribution by following the procedure developed in Ref. [17]. We assume that the Ω baryons are formed from coalescence of three strange quarks of approximately equal momentum and the ϕ mesons from two strange quarks. In the coalescence framework, the Ω baryon production probability is proportional to the local strange quark density, $f_s^3(p_T^s)$, and the ϕ meson is proportional to $f_s(p_T^s)f_{\bar{s}}(p_T^{\bar{s}})$, where f_s ($f_{\bar{s}}$) is the strange (antistrange) quark p_T distribution at hadronization. Assuming that strange quarks and antistrange quarks have a similar p_T distribution, the NCQ-scaled ratio $\frac{N(\Omega^- + \overline{\Omega}^+)|_{p_T^\Omega = 3p_T^s}}{2N(\phi)|_{p_T^\phi = 2p_T^s}}$ could reflect the strange quark distribution at hadronization.

Figure 5(a) shows the NCQ-scaled $\frac{N(\Omega^- + \overline{\Omega}^+)|_{p_T^\Omega = 3p_T^s}}{2N(\phi)|_{p_T^\phi = 2p_T^s}}$ ratios as a function of $p_T^s = p_T/n_q$ at midrapidity ($|y| < 0.5$) from central Au+Au collisions at $\sqrt{s_{NN}} = 11.5$–200 GeV as well as 0–60% collisions at 7.7 GeV. Since the p_T bin widths used for the Ω^- ($\overline{\Omega}^+$) and ϕ meson spectra do not match, we use our Levy fit (see Fig. 1) to interpolate the invariant yield of ϕ meson at desired p_T. The NCQ-scaled $\frac{N(\Omega^- + \overline{\Omega}^+)|_{p_T^\Omega = 3p_T^s}}{2N(\phi)|_{p_T^\phi = 2p_T^s}}$ ratios at all energies can be fit with a Boltzmann distribution

$\frac{g_s A m_T}{T(m_s + T)} e^{-(m_T - m_s)/T}$, where m_s is the effective strange quark mass of 0.46 GeV/c^2 from Ref. [15], m_T is the transverse mass ($\sqrt{m_s^2 + p_T^2}$), and T is the slope parameter of the exponential function which may be related to the freeze-out temperature and radial expansion velocity of strange quarks [28]. Considering different yield ratios of $\bar{s}$ quark over s quark with collision energies, that is, $f_s(p_T^s) = r(\sqrt{s_{NN}})f_{\bar{s}}(p_T^{\bar{s}})$, where $r^3(\sqrt{s_{NN}}) = \frac{dN}{dy}(\overline{\Omega}^+)/\frac{dN}{dy}(\Omega^-)$, we include a correction factor $g_s = (1 + r^3)/r$ in the Boltzmann distribution function (based on the coalescence calculation [14]), and then A is proportional to strange quark rapidity density.

The fitting parameters A and T, and 1σ contours are shown in Fig. 5(b). Figures 5(a) and 5(b) show that the derived strange quark distributions vary little in shape as a function of beam energy from 11.5 to 200 GeV. The amplitude parameter A at 11.5 GeV, however, seems to be noticeably smaller than those data of 19.6 GeV or above. Based on a coalescence model [14], the smaller strange quark local density at 11.5 GeV is probably responsible for the smaller $N(\Omega^- + \overline{\Omega}^+)/[2N(\phi)]$ ratios as shown in Fig. 3, where the first two low p_T points at 11.5 GeV are systematically lower than those at $\sqrt{s_{NN}} \geqslant 19.6$ GeV. At 7.7 GeV, the slope parameter T is smaller than those data of 19.6 GeV or above, with a 1.8σ standard deviation from the 19.6 GeV result. We note that one possible reason for the deviation of T is the centrality difference since the data at 7.7 GeV are for 0–60% while those at other energies are for central collisions. In the framework of the coalescence mechanism, our derived ratio distribution can be sensitive to both the local density and the p_T distribution of strange quarks. Our data of 19.6 GeV or above show little beam energy dependence, suggesting strange quark equilibration may have been approximately achieved in those central collisions, possibly due to strange quark dynamics rather than hadronic processes [31]. The variation of the 11.5 GeV data may arise from the strangeness nonequilibration and the presence of a strangeness phase-space suppression

factor ($\gamma_s < 1$) [28]. A possible transition in the collision dynamics and in the dominant degrees of freedom (partonic versus hadronic) below 19.6 GeV needs further experimental investigations [32].

In summary, STAR has measured the production of multistrange hadrons Ω and ϕ at midrapidity from Au+Au collisions at $\sqrt{s_{NN}} = 7.7$, 11.5, 19.6, 27, and 39 GeV from the BES program at RHIC. The $N(\Omega^- + \overline{\Omega}^+)/[2N(\phi)]$ ratios at intermediate p_T in peripheral collisions are found to be lower than those in central collisions at 19.6, 27, and 39 GeV. The ratios from 11.5 GeV central collisions are systematically lower than those from collisions at 19.6 GeV or above for $p_T > 2.4$ GeV/c. The NCQ-scaled Ω/ϕ ratios show a suppression of strange quark production in 11.5 GeV compared to $\sqrt{s_{NN}} \geqslant 19.6$ GeV. The shapes of the presumably thermal strange quark distributions in 0–60% most central collisions at 7.7 GeV show significant deviations from those in 0–10% most central collisions at higher energies. These features suggest that there is likely a change in the underlying strange quark dynamics in the bulk QCD matter responsible for Ω and ϕ production. Our measurements point to collision energies below 19.6 GeV for further investigation of a possible transition from partonic dominant matter ($\sqrt{s_{NN}} > 19.6$ GeV) to hadronic dominant matter ($\sqrt{s_{NN}} < 11.5$ GeV).

[1] Y. Aoki *et al.*, Nature **443**, 675 (2006).
[2] S. Ejiri, Phys. Rev. D **78**, 074507 (2008); E. S. Bowman and J. I. Kapusta, Phys. Rev. C **79**, 015202 (2009).
[3] M. A. Stephanov, Prog. Theor. Phys. Suppl. **153**, 139 (2004); Z. Fodor and S. D. Katz, J. High Energy Phys. 04 (2004) 050 ; R. V. Gavai and S. Gupta, Phys. Rev. D **78**, 114503 (2008).
[4] C. Blume for the NA49 Collaboration, arXiv:0910.5815.
[5] C. Alt *et al.* (NA49 Collaboration), Phys. Rev. Lett. **94**, 192301 (2005).
[6] D. Elia for the NA57 Collaboration, J. Phys. G **31**, S135 (2005).
[7] C. Alt *et al.* (NA49 Collaboration), Phys. Rev. C **78**, 044907 (2008).
[8] J. Rafelski and B. Müller, Phys. Rev. Lett. **48**, 1066 (1982).
[9] B. I. Abelev *et al.* (STAR Collaboration), Phys. Rev. Lett. **99**, 112301 (2007); Phys. Rev. C **79**, 064903 (2009).
[10] B. Mohanty and N. Xu, J. Phys. G **36**, 064022 (2009); K. J. Wu, F. Liu, and N. Xu, *ibid.* **37**, 094029 (2010); J. Tian, J. H. Chen, Y. G. Ma, X. Z. Cai, F. Jin, G. L. Ma, S. Zhang, and C. Zhong, Phys. Rev. C **79**, 067901 (2009); Md. Nasim, B. Mohanty, and N. Xu, *ibid.* **87**, 014903 (2013).
[11] H. van Hecke, H. Sorge, and N. Xu, Phys. Rev. Lett. **81**, 5764 (1998).
[12] A. Shor, Phys. Rev. Lett. **54**, 1122 (1985).
[13] D. Molnár and S. A. Voloshin, Phys. Rev. Lett. **91**, 092301 (2003).
[14] R. C. Hwa and C. B. Yang, Phys. Rev. C **66**, 025205 (2002); **75**, 054904 (2007).
[15] R. J. Fries, B. Müller, C. Nonaka, and S. A. Bass, Phys. Rev. Lett. **90**, 202303 (2003); Phys. Rev. C **68**, 044902 (2003).
[16] V. Greco, C. M. Ko, and P. Lévai, Phys. Rev. Lett. **90**, 202302 (2003); Phys. Rev. C **68**, 034904 (2003).
[17] J. H. Chen, F. Jin, D. Gangadharan, X. Z. Cai, H. Z. Huang, and Y. G. Ma, Phys. Rev. C **78**, 034907 (2008).
[18] K. Adcox *et al.* (PHENIX Collaboration), Phys. Rev. C **69**, 024904 (2004).
[19] B. I. Abelev *et al.* (STAR Collaboration), Phys. Rev. Lett. **97**, 152301 (2006); Phys. Lett. B **655**, 104 (2007).
[20] G. Agakishiev *et al.* (STAR Collaboration), Phys. Rev. Lett. **108**, 072301 (2012).
[21] B. Abelev *et al.* (ALICE Collaboration), Phys. Rev. Lett. **111**, 222301 (2013).
[22] J. Adams *et al.* (STAR Collaboration), Phys. Rev. Lett. **92**, 052302 (2004).
[23] M. M. Aggarwal *et al.* (STAR Collaboration), arXiv:1007.2613.
[24] J. Cleymans, H. Oeschler, K. Redlich, and S. Wheaton, Phys. Rev. C **73**, 034905 (2006); F. Becattini, J. Manninen, and M. Gaździcki, *ibid.* **73**, 044905 (2006); A. Andronic, P. Braun-Munzinger, and J. Stachel, Nucl. Phys. A **772**, 167 (2006).
[25] K. H. Ackermann *et al.* (STAR Collaboration), Nucl. Instrum. Meth. A **499**, 624 (2003).
[26] L. Adamczyk *et al.* (STAR Collaboration), Phys. Rev. C **86**, 054908 (2012).
[27] L. Adamczyk *et al.* (STAR Collaboration), Phys. Rev. C **88**, 014902 (2013).
[28] J. Adams *et al.* (STAR Collaboration), Phys. Rev. Lett. **92**, 182301 (2004); **98**, 062301 (2007).
[29] J. Adams *et al.* (STAR Collaboration), Phys. Lett. B **612**, 181 (2005); B. I. Abelev *et al.* (STAR Collaboration), *ibid.* **673**, 183 (2009).
[30] T. Hirano, U. Heinz, D. Kharzeev, R. Lacey, and Y. Nara, Phys. Rev. C **77**, 044909 (2008).
[31] P. Koch, B. Müller, and J. Rafelski, Phys. Rep. **142**, 167 (1986).
[32] L. Adamczyk *et al.* (STAR Collaboration), Phys. Rev. Lett. **110**, 142301 (2013).